Journal of Renewable Energies

Revue des Energies Renouvelables

Journal home page: https://revue.cder.dz/index.php/rer

Research Paper

Electrical and Optical Characterization of Non-Hydrogenated a-Si/c-Si Heterojunction Solar Cells

Zoubeida Hafdi *

Département SC_ST, Faculté de Technologie, Université Batna 2, Batna, Algérie.

A R T I C L E I N F O

Article history:
Received 18 May 2021
Accepted 20 December 2021

Keywords:
absorptance, a-Si/c-Si heterojunction, current-voltage characteristics, HIT structure, low cost, non-hydrogenated amorphous silicon.

A B S T R A C T

This work deals with the performance of a heterojunction with intrinsic thin layer solar cell by sputtering silicon on p-type crystalline silicon substrate in argon ambient without hydrogen addition. This first effort was an attempt to use cost-effective means to convert light into electricity and to find fabrication processes which use fewer and cheaper materials for the fabrication of solar cells. Since transport mechanisms of amorphous silicon/crystalline silicon heterojunctions are still under investigation, the aim is to examine the behavior of the fabricated samples under electrical and optical constraints. Initial cell characterization includes electrical behavior via current-voltage characteristics and optical investigation via reflectance and absorptance measurements. Results are analyzed in a tentative to follow the absorption, generation and collection processes in the fabricated cell. The heterojunction interface is found to be a limiting factor in the cell performance. Under sun illumination, the open circuit voltage was 140 mV, the short circuit current was of 6 µA and the fill factor was of 42.56 %. Dark current-voltage characteristics indicated a tunneling and/or recombination carrier transport mechanism, while aborptance/reflectance measurements showed a generation process occurring in most in the crystalline silicon-side of the amorphous/crystalline silicon heterojunction. A carrier collection limitation is a very probable origin of the decreased cell generated current.

* *Corresponding author, E-mail address: hafdiz@yahoo.com*

ISSN: 1112-2242 / E I S S N : 2716-8247

1. Introduction

Algeria is a potential candidate to produce and use renewable energies due to its geographical location. In fact, the energies' sector is being a priority for the public authorities which deploy a great interest to grow and exploit it. The development of this sector requires a new energy consumption model where an important part of renewable energy sources must be attributed. Despite it is trying to acquire the necessary experience for these sources development, several efforts are decisive in term of technological side for solar cells fabrication and efficiency improvement. One of the leading technologies in the solar cells market is the HIT (Heterojunction with Intrinsic Thin layer) solar cell which have gained an increasing attention since Sanyo used this concept in the fabrication of efficient low cost solar cells [1]. Composed of hydrogenated amorphous silicon and crystalline silicon, these heterojunctions combine the low cost and low temperature amorphous silicon fabrication process and the well-known crystalline silicon technology. As a consequence, a rapid industrial growth was observed due this simplified combination. As crystalline silicon is the dominant solar cells fabrication market, high efficiency cells are fabricated in large quantities for microelectronics market. Thin-film solar cells are fabricated using cheaper substrates to reduce the manufacturing cost and increase stability and robustness. Despite this maturity, several questions remain without answer and are still under disagreement concerning the transport mechanisms nature and the passivation effect. For these requirements, several aspects were taken in the design of a HIT solar cell. Some of these aspects are related to the current-voltage characteristics measured at different temperatures, others are inherent of optical properties. In fact, it is sometimes difficult to analyze and interpret measured current-voltage characteristics. One deals with several involved conduction mechanisms which influence the carrier transport. An overview of the dominating transport mechanisms in a-Si/c-Si heterostructures is detailed in [2, 3]. After the publication of HIT solar cells reports which had more than 20% efficiency [4, 5], several experiments were done to study the structure and explain the transport mechanism nature of solar cells with such thin layers [6, 9]. As reported in [10], these works debated that current was mainly dominant by either recombination current or tunneling current depending on temperature, and diffusion current in the crystalline region.

This work is thus dedicated to the manufacture of a HIT solar cell by sputtering silicon on a p-type crystalline silicon substrate without addition of hydrogen. The obtained results are presented and analyzed in terms of electrical characteristics via current-voltage characteristics and optical characteristics where reflectance and absorptance responses were measured in a tentative to follow the absorption, generation and collection processes inside the cell. The paper is organized as follows: in section two, is provided the conducted experimental sequence that was followed in the sample fabrication. In section three, the obtained results and discussion are presented before conclusion is drawn.

2. Experiment

The structure of the fabricated solar cell is illustrated in Fig. 1. 1 cm^2 area wafers were used for the cells fabrication. The substrate is a commercial (111) CZ silicon of 5-20 Ω.cm resistivity and a 500-550 µm thickness. The technological process began by the substrate back-side on which a successive deposition of intrinsic and p-type non-hydrogenated amorphous silicon (a-Si) stacks was performed without breaking the vacuum chamber. This operation was followed by a 100 nm aluminum contact which covered the full cell area. The latter layer acts with the amorphous silicon p+ layer as a back-surface field [11] in order to have a reasonable low contact resistance and to block the minority carriers flow. On the front side of the substrate, intrinsic and n-type non-hydrogenated amorphous silicon stacks were successively deposited also without breaking the vacuum chamber. A layer composed of 75 nm of oxide silicon was evaporated on the n-type amorphous silicon as anti-reflective coating (ARC) for optical improvement of the cell in order to minimize reflection at its surface. Finally, a grid of aluminum contacts of 100 nm thickness was deposited to ensure a decent electrical contact for the solar cell. During e-beam evaporation, the power was adjusted so that the deposition rates were reached. A 13.56 MHz minilab 060 rf magnetron sputtering equipment from Moorefield was used for the stack deposition. A power of 90 W was used to conduct the deposition process without hydrogen addition in all experiments. A high chamber vacuum of ~ 7.29×10^{-7} mbar for back surface stack and ~ 7.66×10^{-7} mbar for front surface stack was set up in a room temperature deposition process to avoid defect creation and doping redistribution representative of high temperature processes [12]. The deposition rates of intrinsic and p-a-Si were, respectively, of 0.60 Å/s and 0.47 Å/s for the back surface stack, and of 0.67 Å/s and 0.86 Å/s for intrinsic and n-a-Si, respectively, for the front surface stack. As inert gas, argon was used in a constant flow of 10 sccm. The working pressure was kept at 1.33×10^{-2} mbar. For back surface aluminum and oxide silicon ARC deposition, a conventional minilab from Moorefield electron beam evaporation system was used. The base pressure was kept at 1.2×10^{-7} mbar, the deposition rate was of 1 Å/s, and the working pressure of 6.5×10^{-7} mbar and 8×10^{-7} mbar, respectively. DC sputtering was used to deposit front surface aluminum. Base and working pressures were

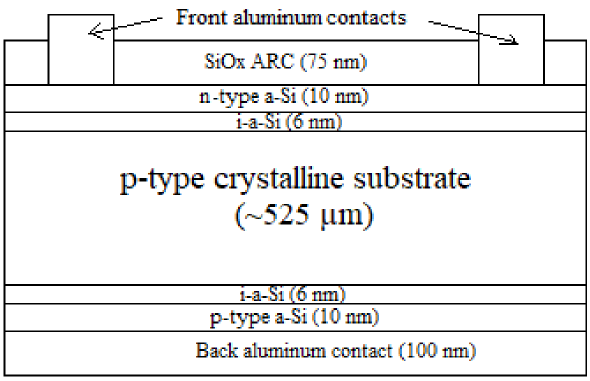

Fig. 1. Fabricated cell structure.

3.9×10^{-7} mbar and 9.37×10^{-3} mbar respectively. The deposition rate was of 0.53 Å/s. The target-to-substrate distance was 14 cm for all measurements. To clean the targets, sputtering was primarily carried out with the shutter closed for several seconds. The measured characteristics are given without post-deposition annealing. The cleaning process began by using commercial detergent and ultrasonic bath. The later includes ethanol (25 min), 90°C heated deionized water rinsing, acetone (25 min) then demineralized water, and finally drying under nitrogen jet. Dip in hydrofluoric acid was used to remove the native oxide immediately before loading the wafers into the deposition chamber. To deposit front aluminum, cleaned metal shadow masks were used for the front metallization. Intrinsic-, n-type-, and p-type silicon targets (purity ~99.999%), SiO_2 crystals (purity ~99.99%) and high pure (99.999%) aluminum were used in the fabrication process. The solar cell performance was characterized by current-voltage measurements in dark and at room temperature using the 4200-SCS source measure unit for semiconductor characterization system and under real conditions of sun illumination. Optical reflectance, absorptance and transmittance were measured using a UV-Visible-NIR spectrophotometer, a Filmetrics F10-RT-UV thin-film analyzer. Figure 2 illustrates sample prototypes of the fabricated HIT solar cells and the metal shadow masks used to deposit front aluminum. It also shows and an initial galvanometer functionality test which reveals the photovoltaic effect.

3. Results and discussion

2.1 Optical Characterization

The deposited films were amorphous in nature. A discussion of this character is established in [13]. The photo-response of the fabricated cell was taken under sun illumination for a load resistance varying from 0 Ω to 10 MΩ. The photovoltaic effect was evident. The illuminated area was 0.928 cm^2.

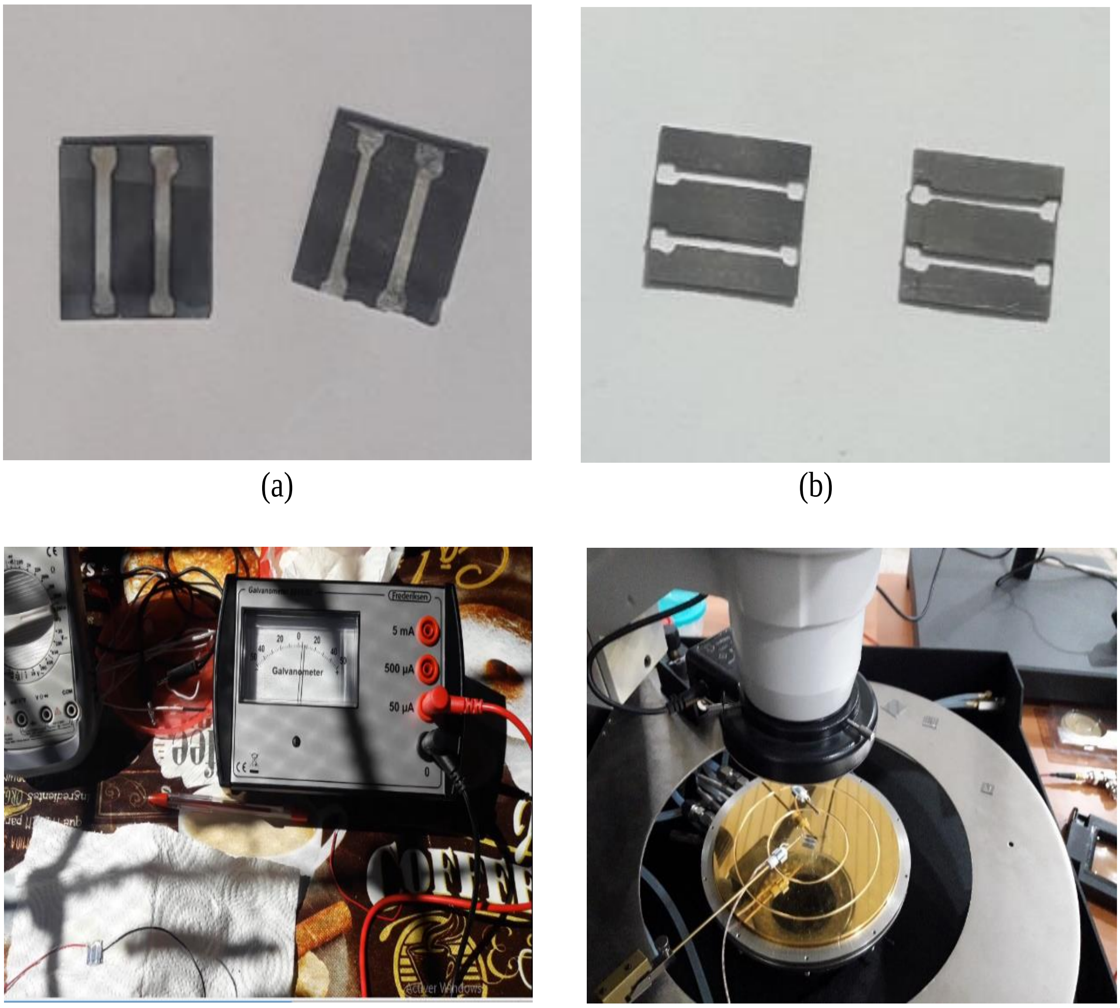

(a) (b) (c) (d)

Fig. 2. Sample prototypes of the fabricated HIT solar cells (a), the metal shadow masks for front aluminum deposition (b), a galvanometer functionality test (c), and cell contact establishing for I-V measurements (d).

An open circuit voltage of 148 mV and a short-circuit current of 6 µA were measured. Despite these low short circuit current and open circuit voltage, the fill factor was 42.56 %. Similar results were reported in [14] where cells having 100 Å of a-Si had low short-circuit current but high fill-factor. This can be attributed to shunt resistance and series resistance mechanisms due to increased recombination in the structure. Effectively, a reduced value of open circuit voltage V_{oc} is usually interpreted as an increase in recombination effects, and as the short-circuit current depends on generation rate and carrier diffusion length, it depends on recombination effects as well. In a tentative to explain this behavior, the optical response of the cell was investigated. The measured absorptance and reflectance exhibited by the solar cell are illustrated in Fig. 3-a. Some corresponding values provided by the spectrophotometer are also shown in Table 1 for illustration. The trends follow those of silicon as illustrated by Fig. 3-b which shows the absorption coefficient of crystalline silicon as a function of wavelength for intrinsic, p-type and n-type silicon with typical bulk doping and emitter doping concentrations, respectively [15]. Corresponding values are added in Table 1 as well.

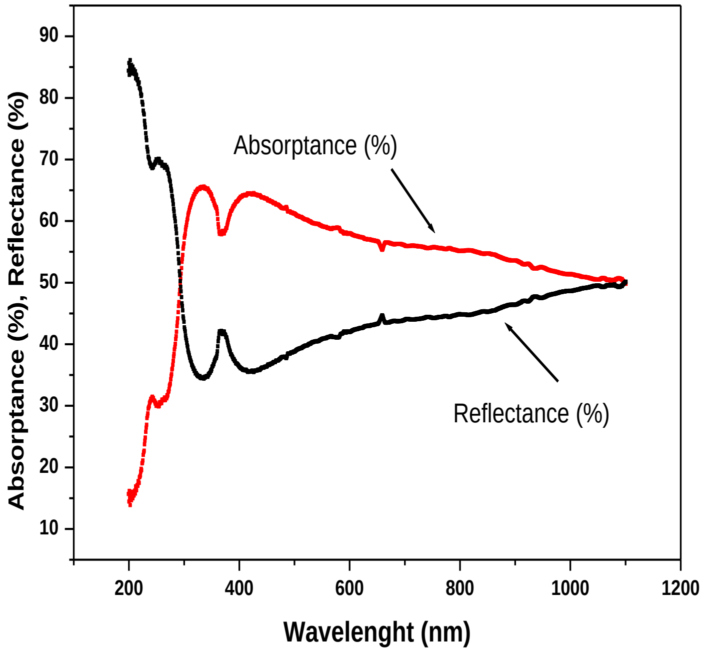

(a)

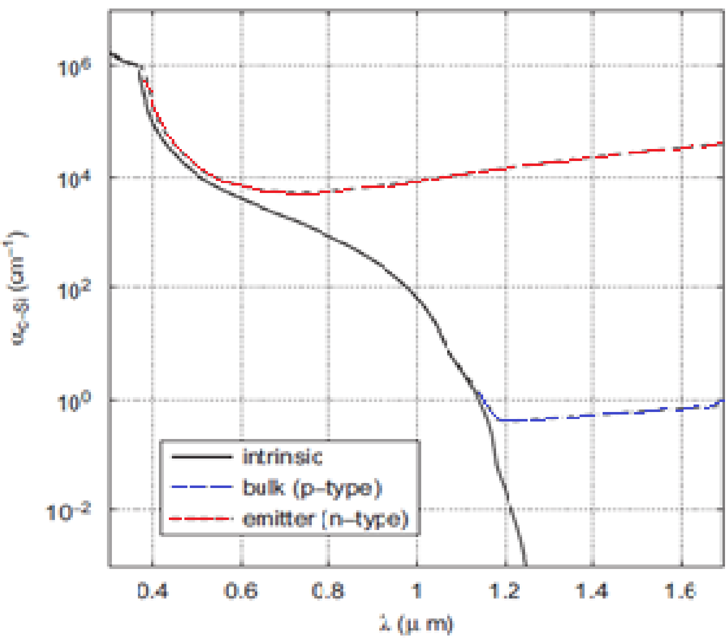

(b)

Fig. 3. (a) Absorptance and reflectance of the cell under study, (b) absorption coefficient of crystalline silicon as a function of wavelength for intrinsic silicon, p-type silicon with typical bulk doping concentration and n-type silicon with typical emitter doping concentration [15].

Table 1. Some values of absorptance and reflectance delivered by the spectrophotometer of the fabricated solar cell, and absorption coefficients for i-, p- and n-type c-Si according to Fig.2 in [15].

Wavelength (nm)	**Absorptance (%)**	**Reflectance (%)**	**i: c-Si absorption coefficient (cm^{-1})**	**p: c-Si absorption coefficient (cm^{-1})**	**n: c-Si absorption coefficient (cm^{-1})**
300,51	57,2871	42,7239	2.2E6	2.2E6	2.3E6
333,89	65,4998	34,5165	1.2E6	1.2E6	1.22E6
334,63	65,5301	34,4937	1.1E6	1.1E6	1E6
335,37	65,4322	34,572	1.05E6	1.05E6	1.05E6
350,12	64,0567	35,929	1E6	1E6	1E6
400,66	63,7066	36,2884	1E5	1E5	2E5
414,5	64,3669	35,6215	2.4E4	2.4E4	1E5
415,23	64,4913	35,4938	2.3E4	2.3 E4	1.1E5
450,04	63,6185	36,3666	1.8E4	1.8E4	2.4E4
500,48	61,2041	38,8003	1E4	1E4	1.1E4
550,59	59,1351	40,8665	6E3	6E3	1E4
600,41	58,0121	41,9873	2.2E3	2.2E3	2.8E3
650,66	56,6882	43,3119	2E3	2E3	2.7E3
700,62	56,0092	43,9925	1.8E3	1.8E3	2.6E3
750,25	55,7249	44,2737	1.3E3	1.3E3	2.5E3
800,2	55,1497	44,8501	1E3	1E3	2.55E3
850,35	54,7594	45,2395	2.6E2	2.6E2	2.7E3
900,59	53,5905	46,4086	2 E2	2 E2	5 E3
950,08	52,4554	47,5441	1.5E2	1.5E2	7E3
1000,6	51,3666	48,6345	8 E1	8 E1	8 E3
1050,53	50,505	49,499	2 E1	2 E1	9 E3
1098,95	49,9719	50,0084	2.6 E0	2.6 E0	1 E4

The transmittance is negligible due to the presence of the back surface aluminum contact leading to a balancing relationship between absroptance and reflectance. According to this figure, the reflectance presents a minimum at 334.63 nm and another at 415.23 nm. At the solar cell front surface, reflectance is important because of reflection losses and optical losses due to the large refractive index of non- hydrogenated amorphous silicon [16]. As the crystalline silicon absorbs light in a wide range of spectrum, the absorptance for larger wavelengths is reduced because of the band gap limitation. The un-hydrogenated amorphous silicon thicknesses that are at least required to lead to a complete photon absorption calculated using the un-hydrogenated amorphous silicon absorption coefficient given in [17] are ~60 nm and ~80 nm, respectively. These depths suggest a predominant absorption in the crystalline silicon side just near the intrinsic a-Si/p type c-Si interface. In [14], a depletion width at zero-bias voltage of 0.6 µm was reported for p type solar cells fabricated by sputtering of 1-10 Ω.cm substrate resistivity. For our 5-20 Ω.cm substrate resistivity, a narrower depletion width of 0.58 µm [13] was found. As known, an increase in doping leads to a narrowing in depletion width which explains the obtained reduced short-circuit current. In other words, as the absorption mainly occurs in the space charge region in the crystalline silicon side, recombination might have occurred before charge collection. The electric field should be weak because the cell emitter is not sufficiently doped (~$7*10^{17}$-10^{18} cm^{-3}) while doping of 10^{20} cm^{-3} [18] is required to get an effective separation and collection high electric field.

2.2 Electrical Characterization

Several conduction mechanisms models describe current-voltage characteristics in a-Si/p-c-Si heterojunctions. Among these mechanisms there are diffusion, emission and recombination. According to any of these models, the current density J and the applied voltage V are related by the following relationship [19]:

$$J \; \alpha \; J_0 e^{(\frac{qV}{nkT})} \tag{1}$$

where J_0 is the saturation current density, k is the Boltzmann's constant, T the measuring temperature, q the elementary charge and n the ideality factor. The later measures how much the cell deviates from the ideal behavior giving an indication on the location where the conduction mechanism occurs and the way in which this mechanism arises. If the transport mechanism is dominated by tunneling, (1) does not hold and it changes to [19]:

$$J = J_0 e^{AV} \tag{2}$$

where A is a constant independent of temperature.

The literature disagrees on the dominant transport mechanism in HIT solar cells for low forward bias region. In fact, an un-hydrogenated a-Si/i-a-Si/c-Si heterostructure is a complex system which uses very small thicknesses of amorphous silicon. It therefore combines several aspects in terms of transport mechanisms. One deals with a set of facts: on one hand, with gap states and lack of passivating hydrogen due to the amorphous silicon material nature and a substrate doping type which highly dictates the dominant transport mechanism, and, on the other hand, with the band offsets which act as barriers, interface states, dipole layers, and discontinuities in bulk properties. Several processes are thus susceptible to arise like tunneling, recombination/generation and thermionic emission. Disagreements concern the activation energies of the low forward bias carrier transport regime which requires another investigation mean, usually the behavior of the saturation current as a function of temperature. While the most part agrees with a tunneling effect [2, 10, 20, 21], the other part predicts a recombination current with an ideality factor of 2 [3, 22]. The investigation of a likely predominant transport mechanism in the structure under study is analyzed through the dark current-voltage (I-V) characteristic at room temperature. The diode-like behavior is shown in Fig. 4 in a semi-log plot for applied voltages varying from -1 V to 1 V. For the analysis of this behavior, it is necessary to determine the values of the saturation current I_s and the ideality factor n in the linear part of the curve. I_s is simply obtained by fitting the semi-log plot of the current as a function of the applied voltage. As can be seen, this operation leads to a one distinguished linear region for direct bias voltages. Deviation from the linear shape for higher applied voltages occurs at about 0.65V. This deviation is known to be caused by series resistance. A junction current-voltage plot showing a slope change at an applied voltage range, suggests that a different conduction process starts to dominate from this voltage range. Several studies on a-Si/c-Si heterojunctions reported the presence of distinct voltage regions corresponding, each of them, to a particular mechanism of electronic transport depending on the ideality factor. In our case, the solar cell exhibits, besides this deviation, a low current level induced by a degradation in the a-Si/c-Si interface [13]. Series resistance which reflects material and electrodes resistivity, and metal/Si contact is thus high. As a consequence, it limits the current at high-forward bias regime. The calculated ideality factor n was of 5.53 for direct bias voltages and the saturation current was of 4.72×10^{-8} A. With an ideality factor greater than two it is difficult to relate the I-V behavior to a specific transport mechanism without temperature effect investigation. In fact, carrier transport in heterojunctions, as for any semiconductor device, depends not only on temperature, but on bias applied voltage and the component structure as well. To predict the electronic transport using I-V characteristics analysis, it was showed that the saturation current and the related exponential factor A depend on temperature according to the appropriate model. It is therefore useful to use another mean, generally the value of the ideality factor and the temperature dependence of the saturation current density. The Arrhenius plot (log J_0 vs 1/T) allows the determination of the activation energy which helps, in turn, to distinguish the numerous mechanisms. As can be seen, the ideality factor deviates roughly from the values in the literature. Usually, values of n fall between 1 and 2. But values greater than 2 were also reported and analyzed. In [23], recombination of the carriers at the junction are caused by defects that exist in the quasi-neutral region and in the junction which results in high values of ideality factor. Reference [24], for the interpretation of the commonly observed I-V characteristics of crystalline silicon solar cells showing ideality factor larger than two, revealed that the dark I-V behavior usually deviate from that expected by the classical diode theory by an unusually high ideality factor and magnitude at biases smaller than about 0.5 V. It indicated that the recombination current is flowing preferentially in certain local extended defect positions like the edge or local shunts. For the cell under study, the obtained small slope (high ideality factor) can be explained by tunneling since this effect strongly depends on the density of localized states in the amorphous silicon layer [10]. This density was non negligible as estimated by capacitance-voltage measurements [13]. The computed value was of 6.93 10^{14} cm^{-3} for a substrate doping of N_A~2.10^{15} cm^{-3} [13]. For the same reason, carrier recombination can also be a non-negligible component of the I-V behavior as shown above by optical characterization.

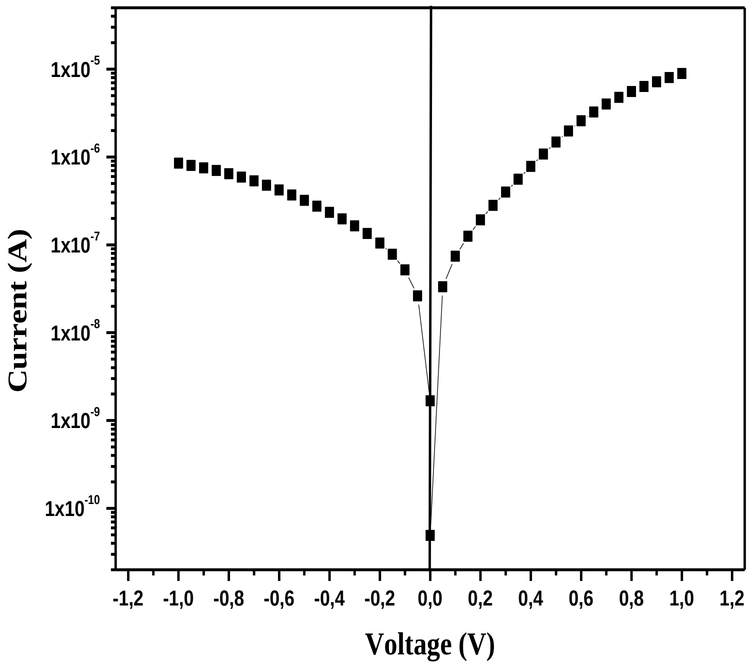

Fig. 4. Dark current-voltage characteristic of the fabricated solar cell.

4. Conclusions

In this work, a HIT solar cell was fabricated by rf magnetron sputtering method on a p-type crystalline silicon wafer in argon ambient without addition of hydrogen. The behavior of the obtained non-hydrogenated amorphous silicon/p type crystalline silicon heterojunction HIT solar cell was investigated. Analysis of the dark current-voltage behavior in association of earlier obtained capacitance-voltage measurements showed that recombination and/or tunneling seem to competitively govern carrier transport across the heterojunction. Cell photo-response indicates that the major absorption takes place in the crystalline silicon side of the heterojunction. From technological side, further work is needed to improve the cell fabrication, namely the intrinsic a-Si/p c-Si interface properties, and to be accurate on the dominant conduction mechanism in a-Si/c-Si heterojunction.

5. Acknowledgements

The author would like to thank A. Bendjerad and A. Saidi for their help in deposition operation and sample preparation.

6. References

[1] Tanaka M, Taguchi M, Matsuyama T, Sawada T, Tsuda S, Nakano S, Hanafusa H, Kuwano Y. Development of new a-Si/c-Si Heterojunction Solar Cells: ACJ-HIT (Artificially Constructed Junction-Heterojunction with Intrinsic Thin-Layer). Jpn. J. Appl. Phys. 2015;31:3518-3522. doi:10.1143/JJAP.31.3518.

[2] Schulze TF, Korte L, Conrad E, Schmidt M, Rech B. Electrical transport mechanisms in a-si:h/c-si heterojunction solar cells. J. Appl. Phys. 2010; 107:023711-1-023711-13. doi:10.1063/1.3267316.

[3] Marsal LF, Pallares J, Correig X, Calderer J, Alcubillan R. Electrical characterization of n-amorphous/p-crystalline silicon heterojunctions. J. Appl. Phys. 1996; 79:8493–8497. doi:10.1063/1.362526.

[4] Mishima T, Tagushi M, Sakata H, Maruyama E. Development status of high-efficiency HIT solar cells, Sol. Energy Mater. Sol. Cells. 2011; 95:18-21. doi: 10.1016/j.solmat.2010.04.030.

[5] Tagushi M, Yano A, Tohoda S, Matsuyama K, Nishiwaki T, Fujita K, Maruyama E. 24.7% record efficiency HIT solar cell on thin silicon wafer. IEEE J. Photovoltaic. 2014; 4:96-99. doi:10.1109/jphotov.2013.2282737.

[6] Lin JT, Lai CC, Lee CT, Hu YY, Ho KY, Haga SW. A high-efficiency HIT solar cell with pillar texturing, IEEE J. Photovoltaics. 2018; 8:669-675. doi:10.1109/jphotov.2018.2804330.

[7] Lin JT, Lee CT, Chen WH, Haga SW. Hu YY, Ho KY. Double-sided symmetrical and crossed emitter crystalline silicon solar cells with heterojunctions for bifacial applications. IEEE J. Photovoltaic. 2018; 8:441-447. doi:10.1109/jphotov.2018.2790798.

[8] Kumar M, Kumar A. Performance assessment of different photovoltaic technologies for canal-top and reservoir applications in subtropical humid climate. IEEE J. Photovoltaics. 2019; 9:722-732. doi:10.1109/jphotov.2019.2892520.

[9] Jordan DC, Deline C, Johnston S, Rummel SR, Sekulic B, Hacke P, Kurtz SR, Davis KO, Schneller EJ, Sun X, Alam MA, Sinton RA. Silicon heterojunction system field performance. IEEE J. Photovoltaics. 2018; 8:177-182. doi:10.1109/jphotov.2017.2765680.

[10] M, E. Maruyama E, Tanaka M. Temperature dependence of amorphous/crystalline silicon heterojunction solar cells, Jpn. J. Appl. Phys. 2008; 47:814–818. doi:10.1143/jjap.47.814.

[11] Ferdiansjah, Faridah D, Mularso KT. Analysis of back surface field (BSF) performance in p-type and n-type monocrystalline silicon wafer. Int. Energy Conf., Yogyakarta, Indonesia, 2018;43:1-4. doi:10.1143/jjap.47.81410.1051/e3sconf/20184301006.

[12] Lohner T, Serényi1 M, Basa DK, Khánh NQ, Nemcsics Á, Petrik P, Turmezei P. Composition and thickness of rf sputtered amorphous silicon alloy films. Acta Polytech. Hungarica. 2008;5:23-30.

[13] Hafdi Z. On capacitance-voltage characteristics of non-hydrogenated amorphous silicon heterojunctions for Solar-cell applications. Materials Today: Proceedings. 2020;33:1934-1938. doi:10.1016/j.matpr.2020.05.790.

[14] Jagannathan B, Anderson WA, Coleman J. Amorphous silicon/p-type crystalline silicon heterojunction solar cells, Sol. Energy Mater. Sol. Cells. 1997 ;46 :289-310. doi:10.1016/S0927-0248(97)00012-3.

[15] Santbergen R, van Zolingen RJC. The absorption factor of crystalline silicon PV cells: a numerical and experimental study. Sol. Energy Mater. Sol. Cells. 2008;92:432-444. doi:10.1016/j.solmat.2007.10.005.

[16] Bouchut P, Chenevas-Paule A. Influence de l'hydrogène sur les propriétés optiques du silicium amorphe Rhe, J. Phy. Colloques. 1981;42:C1-439-C1-451. doi:10.1051/jphyscol:1981134.

[17] Knief S, von Niessen W. Disorder, defects, and optical absorption in a−Si and a−Si: H. Phys. Rev. B. 1999;59:12940-12946. doi:10.1103/PhysRevB.59.12940.

[18] Ghannam M, Abdulraheem Y. Fundamental constraints imposed by energy barriers on the fill factor and on the efficiency of silicon heterojunction solar cells. Sol. Energy Mater. Sol. Cells. 2017;171:228-238. doi:1016/j.solmat.2017.06.042.

[19] Matsuura H, Okuno T, Okushi H, Tanaka K. Electrical properties of n-amorphous/p-crystalline silicon heterojunctions. J. Appl. Phys. 1984;55:1012-1019. doi:10.1063/1.333193.

[20] Jagannathan B, Anderson WA. Interface effects on the carrier transport and photovoltaic properties of hydrogenated amorphous silicon/crystalline silicon solar cells. Sol. Energy Mater. Sol. Cells. 1996;44:165-176. doi:10.1016/0927-0248(96)00042-6.

[21] Dao VA, Lee Y, Kim S, Kim Y, Lakshminarayan N, Yi J. Interface characterization and electrical transport mechanisms in a-si:H/c-si heterojunction solar cells. J. Electrochem. Society. 2011;158:H312–H317. doi:10.1149/1.3534202.

[22] Marsal LF, Martin I, Pallares J, Orpella A, Alcubilla R. Annealing effects on the conduction mechanisms of p^+ -amorphous-$Si_{0.8}C_{0.2}$:H/n-crystalline-Si diodes. J. Appl. Phys. 2003;94:2622–2626. doi:10.1063/1.1591073.

[23] Perny M, Saly V, Mikolášek M, Vary M, Huran J. Solar cell heterojunction a-SiC:H/c-Si structure under dark and illumination. *Proc.* EPE, Kouty nad Desnou, Czech Republic, 2015. doi:10.1109/EPE.2015.7161115.

[24] Breitenstein O, Altermatt P, Ramspeck K, Green MA, Zhao J, Schenk A. Interpretation of the commonly Oobserved I-V characteristics of C-SI Cells having ideality factor larger than two. 4th World Conference on Photovoltaic Energy Conference, Waikoloa, HI, USA, 2006. doi:10.1109/WCPEC.2006.279597.